Dynamics of a plant–herbivore model

Yun Kang , Dieter Armbruster & Yang Kuang

Submit your article to this journal

View related articles

Dynamics of a plant–herbivore model

Yun Kang, Dieter Armbruster* and Yang Kuang

Department of Mathematics and Statistics, Arizona State University, Tempe, AZ, USA

We formulate a simple host–parasite type model to study the interaction of certain plants and herbivores. Our two-dimensional discrete-time model utilizes leaf and herbivore biomass as state variables. The parameter space consists of the growth rate of the host population and a parameter describing the damage inflicted by herbivores. We present insightful bifurcation diagrams in that parameter space. Bistability and a crisis of a strange attractor suggest two control strategies: reducing the population of the herbivore under some threshold or increasing the growth rate of the plant leaves.

Keywords: host–parasite model; plant–herbivore model; bifurcation; chaos; control strategies

AMS Subject Classifications: 34K20; 92C50; 92D25

1. Introduction

The usual framework for discrete-generation host–parasite models has the form

$$P_{n+1} = \lambda P_n f(P_n, H_n), \tag{1}$$

$$H_{n+1} = c\lambda P_n \left[1 - f(P_n, H_n)\right], \tag{2}$$

where P and H are the population biomasses of the host (a plant) and the parasite (a herbivore) in successive generations n and $n + 1$, respectively, λ is the host's inherent rate of increase ($\lambda = e^r$ where r is the intrinsic rate of increase) in the absence of the parasites, c is the biomass conversion constant and f is the function defining the fractional survival of hosts from parasitism. Throughout the rest of this paper, n takes nonnegative integer values.

The simplest version of this model is that of Nicholson [13] and Nicholson and Bailey [14] who explored in-depth a model in which the proportion of hosts escaping parasitism is given by the zero-term of the Poisson distribution namely,

$$f(P_n, H_n) = e^{-aH_n}, \tag{3}$$

where a is the mean encounters per host. Thus, $1 - e^{-aH_n}$ is the probability of a host will be attacked. Substituting Equation (3) into the Equations (1) and (2) gives:

$$P_{n+1} = \lambda P_n e^{-aH_n}, \tag{4}$$

$$H_{n+1} = c\lambda P_n \left[1 - e^{-aH_n}\right]. \tag{5}$$

*Corresponding author. Email: armbruster@asu.edu

When $\lambda > 1$, the Nicholson–Bailey model has a positive equilibrium, which is unstable [7].

Beddington et al. [3] considered the following modified Nicholson–Bailey model

$$P_{n+1} = \lambda P_n e^{\left(-\frac{rP_n}{P_{\max}} - aH_n\right)}, \tag{6}$$

$$H_{n+1} = c\lambda P_n \left(1 - e^{-aH_n}\right), \tag{7}$$

where $P_{\max}$ is the so-called environment imposed 'carrying capacity' for the host in the absence of the parasite. What was an unstable positive equilibrium when no density-dependent is assumed for host population growth becomes locally stable for a large set of parameter values [3]. For other parameter values, the model can generate attractors of various complexity, ranging from a set of limit cycles of various periods to strange and chaotic ones.

Observe that the structure of Equations (6) and (7) implies that the host density-dependence acts at a particular time in their life cycle in relation to the stage attacked by the parasites. The H_n herbivores search for P_n hosts *before* the density-dependent growth regulation takes effect. Hence, the next generation of herbivores depends on P_n, the initial host population prior to parasitism. This leads to the following general form:

$$P_{n+1} = \lambda P_n g(P_n) f(H_n), \tag{8}$$

$$H_{n+1} = c\lambda P_n \left[1 - f(H_n)\right], \tag{9}$$

where $f(H_n)$ represents the fraction of hosts surviving parasitism, and the host density dependence takes the form $g(P_n) = e^{(1 - rP_n/P_{max})}$.

In many observable plant–herbivore (host–parasite) interactions, herbivores (parasites) are not attracted to and attack plants until their leaves form good canopies. Moreover, the feeding process continues throughout most periods of the growing season. This argues for plant–herbivore (host–parasite) models where the herbivory (parasitization) occurs *after* the density-dependent growth regulation of the host takes place. The importance of the sequencing of events when constructing discrete-time models is well known [5,7]. We propose the following discrete models for such plant–herbivore interactions:

$$P_{n+1} = \lambda P_n g(P_n) f(H_n), \tag{10}$$

$$H_{n+1} = c\lambda P_n g(P_n) \left[1 - f(H_n)\right]. \tag{11}$$

May [11] introduced Equations (10) and (11). Here we assume that the consumed plant biomass is fully converted to herbivore biomass, *i.e.* model (10) and (11) observes the conservation of biomass production. This basic conservation law is often ignored in existing population models without proper justification.

2. A general plant–herbivore model and its boundary dynamics

In the following, we apply the above model framework to the interaction between a plant species and a herbivore species. We are motivated by the gypsy moth, which is a notorious forest pest in North Central United States whose outbreaks are almost periodic and cause significant damage to the infested forests. In our discrete-time model, we assume that herbivore population growth is a nonlinear function of herbivore feeding rate, and that plant population growth decreases gradually with increasing herbivory. Also, in the absence of the herbivore, plant population density is regulated by intraspecific competition [2,9,16], so we allow for density dependence in the plant. We model the plant and herbivore dynamics through their biomass changes. We assume that the

soil acts as an unlimited reservoir for biomass growth. A plant takes up the nutrient from the soil and stores the nutrient in its stem, bark, twig and leaves. During spring, leaves emerge in a deciduous forest. A herbivore in our model has a one year life cycle, like the insects. For example, the gypsy moth larvae hatch from the egg mass after bud-break and feed on new leaves. At the end of the season n, adult gypsy moths lay eggs and die. We make the following assumptions:

ASSUMPTION 1   *P_n represents the plant population's (nutritious) biomass after the attacks by the herbivore but before its defoliation. H_n represents the biomass of the herbivore before they die at the end of the season n.*

ASSUMPTION 2   *Without the herbivore, the biomass of the plant population follows the dynamics of the Ricker model [15],*

$$P_{n+1} = P_n e^{r[1-P_n/P_{\max}]},\tag{12}$$

with a constant growth rate r and plant carrying capacity $P_{\max}$. The Ricker dynamics determines the amount of new leaves available for consumption for the herbivore.

ASSUMPTION 3   *We assume that the herbivores search for food randomly. The leaf area consumed is measured by the parameter a, i.e., a is a constant that correlates the total amount of the biomass that an herbivore consumes. The herbivore has a one year life cycle, the larger a, the faster the feeding rate.*

After attacks by herbivores, the biomass in the plant population is reduced to a fraction $e^{-aH(n)}$ of that present in the absence of herbivores. Hence,

$$P_{n+1} = P_n e^{r[1-P_n/P_{\max}]-aH_n}.\tag{13}$$

The amount of decreased biomass in the plants is converted to the biomass of the herbivore. *Mathematically, the conversion parameter can be scaled away by a simple change of variable $H_n/c \to H_n$.* Hence, for convenience, we assume below that the biomass conversion parameter is 1. Therefore, at the end of the season n, we have

$$H_{n+1} = P_n e^{r[1-P_n/P_{\max}]}\left[1 - e^{-aH_n}\right].\tag{14}$$

In nature, densities of the host plants are usually high for long periods, during which insect densities are correspondingly low. Periods of high plant abundance are punctuated by sudden insect outbreaks, followed by a rapid crash and rapid recovery of the host plant [4,6,12]. The system (13) and (14) captures these dynamics [1]. There are three parameters in our system r, a and $P_{\max}$. We can scale $P_{\max}$ away by setting $x_n = P_n/P_{\max}, y_n = H_n/P_{\max}, a \to aP_{\max}$. This yields the following non dimensionalized system:

$$x_{n+1} = x_n e^{r[1-x_n]-ay_n},\tag{15}$$

$$y_{n+1} = x_n e^{r[1-x_n]}\left[1 - e^{-ay_n}\right].\tag{16}$$

It is easy to see that if $x_0 = 0$ ($y_0 = 0$), then $x_n = 0$ ($y_n = 0$) for $n > 0$. We assume that $a > 0$ and $r > 0$. Observe that $x_{n+1} + y_{n+1} = x_n e^{r(1-x_n)} \le e^{r-1}/r$. We thus have the following propositions:

PROPOSITION 2.1   *Assume that $a > 0, r > 0, x_0 > 0$ and $y_0 > 0$, then $x_n > 0$ and $y_n > 0$ for all $n > 0$. In addition, we have $\max_{n\in Z^+}\{x_n, y_n\} \le e^{r-1}/r$ for $n > 0$.*

The exponential nonlinearity in Ricker-type models is a prototype for an ecological model describing discrete-time populations with a one hump dynamics. One hump dynamics indicate an optimal population size that maximizes reproductive success – deviations from which lead to reduced populations in the next generation. This reflects limitations to population growth at high densities such as limited food, water or space [1].

The system (15) and (16) has the two boundary equilibria $(0, 0)$ and $(1,0)$ and possibly multiple interior equilibria depending on the parameter values of r and a.

At the boundary equilibrium point $(0, 0)$, the Jacobian matrix takes the form of

$$J|_{(0,0)} = \begin{bmatrix} e^r & 0 \\ 0 & 0 \end{bmatrix} \tag{17}$$

with eigenvalues $\lambda_1 = e^r \geq 1$ and $\lambda_2 = 0 < 1$. Hence, the origin is a saddle, which is stable on the y-axis and unstable on the x-axis. This implies that plants cannot die out.

At the boundary equilibrium point $(1, 0)$, the Jacobian matrix is

$$J|_{(1,0)} = \begin{bmatrix} 1 - r & -a \\ 0 & a \end{bmatrix} \tag{18}$$

with eigenvalues $\lambda_1 = 1 - r$ and $\lambda_2 = a$. As a result, we have two codimension-one bifurcations from this equilibrium:

- Near $r = 2$ and $a \neq 1$, the Taylor expansion of Equation (15) on the invariant manifold $y = 0$ gives

$$u_{n+1} = (-1 - \gamma)u_n + \frac{2u_n^3}{3} \tag{19}$$

where $\gamma = r - 2$ and $u_n = x_n - 1$. Equation (19) satisfies the necessary and sufficient conditions for period doubling [17] consistent with the Ricker dynamics.
- Near $a = 1$ and $r \neq 0, 2$, we can perform a center manifold reduction and obtain the equation (if $r = 2$ then our system has a codimension-two bifurcation).

$$v_{n+1} = (1 + \alpha)v_n - \frac{(\alpha + \gamma)v_n^2}{2} - \frac{v_n^3}{3} \tag{20}$$

where $\gamma = r - 2, \alpha = a - 1$ and $v_n = y_n$. For $\gamma \neq 0$, Equation (20) satisfies the necessary and sufficient conditions for a transcritical bifurcation. For $\alpha = \gamma = 0$, we have a pitchfork bifurcation.
- We can unfold the transcritical bifurcation to obtain a saddle-node bifurcations at

$$v = \sqrt{-3\alpha}, \quad \gamma = -\frac{4}{3}\sqrt{-3\alpha} - \alpha, \tag{21}$$

$$v = -\sqrt{-3\alpha}, \quad \gamma = \frac{4}{3}\sqrt{-3\alpha} - \alpha. \tag{22}$$

Notice that the equilibrium (22) lies in the second quadrant and hence is biologically uninteresting. Equilibrium (21) exists only when $\alpha < 0$.
- When $r = 2$ and $a = 1$, we have the most degenerate case with eigenvalues $\lambda_1 = -1$ and $\lambda_2 = 1$.

3. Interior equilibria

Let $E = (x^*, y^*)$ be an interior equilibrium of model (15) and (16). From Equation (15), we obtain $x^* = 1 - ay^*/r$ and from Equation (16), we obtain $x^* = y^*/(e^{ay^*} - 1)$ (since $ay^* = r(1 - x^*)$).
Let

$$f_1(y) = 1 - \frac{ay}{r} \quad \text{and} \quad f_2(y) = \frac{y}{e^{ay} - 1}.$$

Then the interior equilibria are the intersection points of these two functions in the first quadrant Q^+.

Clearly, $f_1(y)$ is a decreasing linear function. It is easy to show that $f_2(y)$ is also decreasing. In addition, we have $\lim_{y \to 0} f_2(y) = 1/a$ and $\lim_{y \to 0} f_2'(y) = -1/2$. Observe that if $a = 1, r = 2$, $f_1(y)$ and $f_2(y)$ are tangent at the boundary equilibrium $(1, 0)$ with a slope of $-1/2$. Straight-forward computation shows that $f_2''(y) \geq 0$ and $f_2'(y) \in (-1/2, 0)$, for $y > 0$. Hence, the intersection of $f_1(y)$ and $f_2(y)$ in the first quadrant Q^+ has 0 (Figure 1a), 1 (Figure 1b) or 2 (Figure 1c) interior equilibria.

Parameter r measures growth rate of plants and a measures average area of leaves consumed by a herbivore. If r, a are relatively small, for instance, $a < 1$ and $r < 2$, then herbivores die out because of either not enough food for consumption or the herbivore consumption rate is not high enough. This is the essence of the following proposition.
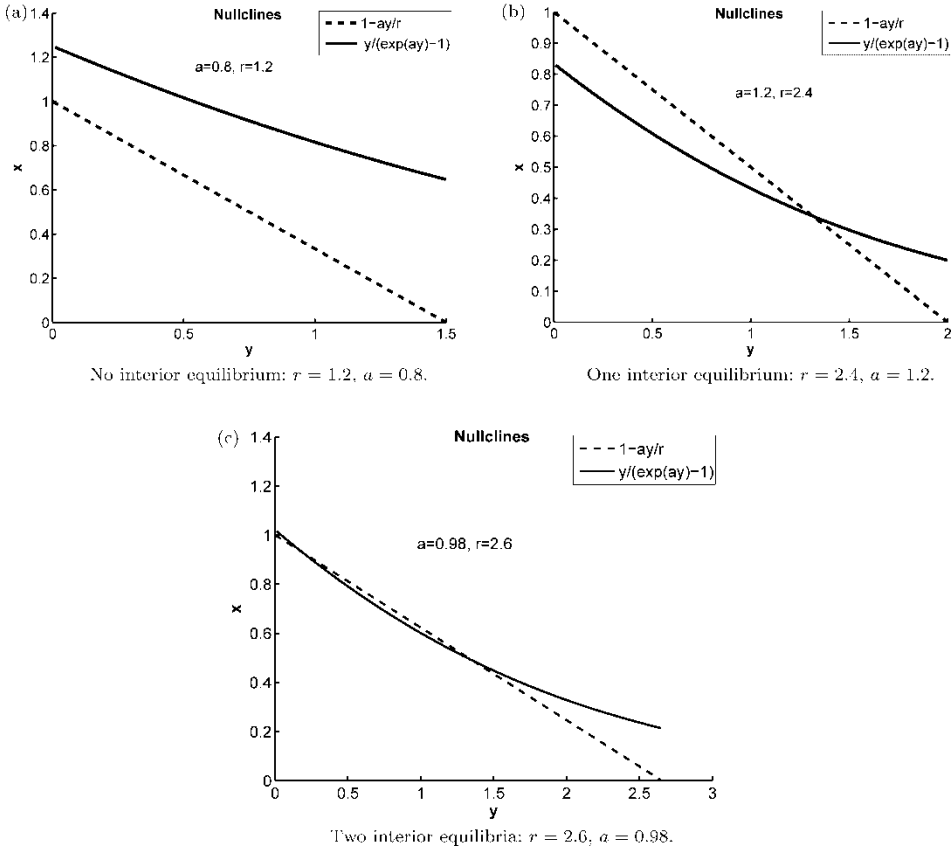

Figure 1. Interior equilibria.

PROPOSITION 3.1   *For $0 < r < 2$, $0 < a < 1$, model* (15) *and* (16) *has no positive equilibrium* (*Figure* 1*a*).

Proof   We note that if $0 < a < 1$, $0 < r < 2$ and $y \geq 0$, then

$$F(y) = f_2(y) - f_1(y) = \frac{y}{e^{ay} - 1} + \frac{ay}{r} - 1 = \frac{N(y)}{e^{ay} - 1},$$

where

$$N(y) = y + \frac{ay}{r}(e^{ay} - 1) - (e^{ay} - 1).$$

Since $0 < a < 1$, we see that $N(0) = 0$, $N'(0) = 1 - a > 0$. Since $0 < r < 2$, we see that $N''(y) = a^2 e^{ay}(ay/r + 2/r - 1) > 0$. Hence, $F(y) > 0$, $y \in R^+$. This shows that model (15) and (16) has no positive equilibrium points.   ∎

If herbivores consume the plant at a faster rate, *e.g.*, $a > 1$, which amounts to saying that herbivores eat enough food during their growth season, then the following proposition suggests that herbivores may persist.

PROPOSITION 3.2   *For $a > 1$, model* (15) *and* (16) *has an unique positive equilibrium* (*Figure* 1*b*).

Proof   For $a > 1$, we see that $f_2(0) < f_1(0)$. Moreover, $f_2'(y) \in (-1/2, 0)$, $f_2''(y) \geq 0$, $f_1'(y) = -a/r$ and $f_2(r/a) > f_1(r/a) = 0$.   ∎

By the Jury test [7], we see that the interior equilibrium is locally asymptotically stable if

$$2 > 1 + \det(J) = 1 + ax^*(1 - rx^*)e^{ay^*} > |\mathrm{tr}(J)| = |1 + (a - r)x^*|. \tag{23}$$

The biological implication of inequality (23) is simple: if it holds, then the plant-herbivore interaction exhibit simple stable steady state dynamics. However, it is not clear what biologically mechanisms ensure that the inequalities in (23) holds, since the dynamical outcomes are very sensitive to the two parameters r and a (Figure 2).

3.1.   *Codimension one: Neimark–Sacker bifurcation*

The condition for a Neimark–Sacker bifurcation is that $\lambda \cdot \bar{\lambda} = 1$ and λ is not a real number. This translates into the three equations

$$r(1 - x) - ay = 0, \tag{24}$$

$$x(e^{ay} - 1) = y, \tag{25}$$

$$a(1 - rx)(x + y) = 1, \tag{26}$$

and the inequality

$$|1 + (a - r)x| < 2. \tag{27}$$

Equations 24–26 cannot be solved in closed form but it is easy to solve them numerically for x and y values in the first quadrant. It is easy to check that the Trace condition (23) is always satisfied for those values of x and y. The curve drawn with small circles in Figure 2 that forms the boundary between region 6 and 7 depicts the numerical solutions for these equations and hence represents the codimension one parameter set for the Neimark–Sacker bifurcation.
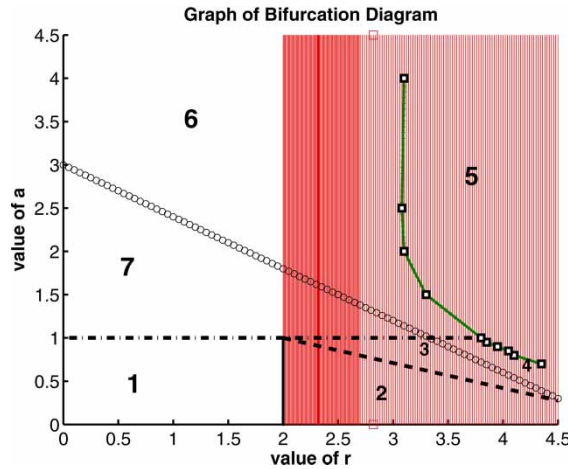
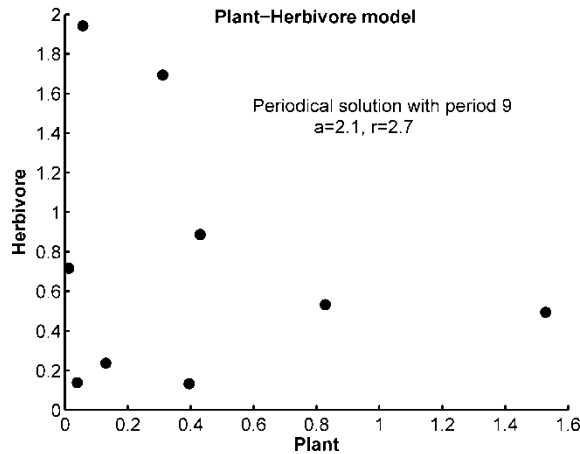Figure 2. Bifurcation diagram of parameters r and a.

Figure 3. Periodic solution with period 9 for $r = 2.7$, $a = 2.1$.

Neimark–Sacker bifurcations generate dynamically invariant circles. As a result, we may find isolated periodic orbits as well as trajectories that cover the invariant circle densely. Figure 3 shows a period 9 orbit while Figure 4 illustrates a dense orbit resembling an invariant circle.

There exists no bifurcation with codimension higher than one in the interior of parameter space (r, a) except the point $(2, 1)$. The most degenerated case occurs at the boundary equilibrium $(1, 0)$, which simultaneously undergoes a pitchfork and a period doubling bifurcation at $(r, a) = (2, 1)$.

3.2. *Bifurcation diagram in the (r, a) – parameter space*

The codimension-one bifurcations discussed in Section 3.1 allow us to determine regions in parameter space r and a for which the dynamics of the system are topologically equivalent. Figure 2 shows the relevant (r, a) space.

Recall that the dynamics on the invariant manifold $y = 0$ is a unimodal map (the Ricker model) yielding a period doubling cascade to chaos as the parameter r is increased [8]. In Figure 2, the parameter region for which the equilibrium in the Ricker model is stable ($r < 2$) is *to the left of*
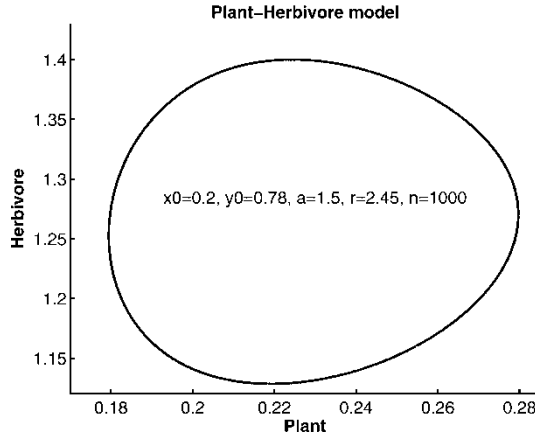
Figure 4.   Dense orbit in phase space for $r = 2.45$, $a = 1.5$.

shaded region. The parameter region exhibiting stable periodic orbits in the Ricker model defined by $2 \leq r < r_c$ is indicated by a *a strong shaded region*. For $r > r_c$, the Ricker model generates progressively more complex dynamics including chaotic behaviour (*light shading*). In addition, Figure 2 shows the following codimension-one curves.

(1) The transcritical bifurcation at $a = 1$ is shown as a dashed-dotted line.
(2) The saddle-node bifurcation emanating from the pitchfork bifurcation at $a = 1, r = 2$ is drawn dashed. Only the part that leads to a saddle-node bifurcation in the first quadrant is shown.
(3) The Neimark–Sacker bifurcation generated numerically is shown as circles.
(4) The black line connects simulations shown as *small rectangles* representing values of r and a when a strange attractor collapses. The line approximately indicates the collapse of a strange attractor through a crisis.

These bifurcation curves divide the parameters space (r, a) into seven regions labelled one to seven in Figure 2.
    Our simulation results suggest the following:

(1) The boundary equilibrium $(1, 0)$ is a globally stable attractor for $0 < r < 2, 0 < a < 1$. In this parameter region, herbivores cannot coexist with plants. The biological interpretation for this is that both values of r, a are relatively small, which implies that either the plant cannot produce enough food for the herbivores because of the small growth rate r or the herbivores' feeding rate a is too small to provide enough food for its persistence.
(2) The system has no interior equilibrium and the Ricker dynamics is globally attracting to either periodic orbits or to chaotic orbits on the x-axis. While the value of r producing such dynamics is larger than the values producing the simple global dynamics described in (1), it cannot compensate the small value of a, leading to the demise of the herbivores.
(3) Further increasing the plant growth rate enables the system to gain two interior equilibria. The one with the larger y-value is stable. The boundary equilibrium is still stable with respect to perturbations into the y-direction. In this case, the value of r is large enough to compensate for the low herbivore feeding rate.
(4) The stable interior equilibrium loses stability through a Neimark–Sacker bifurcation. We numerically find stable periodic orbits (isolated and dense) for some moderate values of r and a, and strange attractors for larger values of r and a.

(5) The transition between region 4 and the region 5 is the numerically generated curve where the strange attractor collapses in a crisis bifurcation. Inside region 5, there is no attractor in the interior of the phase space. All interior points are attracted to x-axis which exhibits mostly chaotic dynamics.

(6) The system has only one interior equilibrium which is unstable. There is an invariant loop around the unstable interior equilibrium. As the values of r and a increase, that invariant loop becomes unstable and forms a strange attractor. The transition between the region 6 and the region 7 is again through a Neimark–Sacker bifurcation.

(7) The system has a stable interior equilibrium which appears to be the global attractor. Herbivores can consume enough food to coexist with plant. The transition between the regions 5, 6, 7 and the regions 1, 2, 3, 4 is a transcritical bifurcation.

4. Bistability and chaos

In the following two subsections, we focus on the frequently observed dynamics: bistability and chaos.

4.1. *Bistability*

Theorem 4.1 below implies that when model (15) and (16) has an attractor in the interior of the phase space, and $a < 1$, it produces bistability between the attractor in the interior and the attractor on the x-axis. This is true for regions 3 and 4 where we have stable interior attractors (equilibria, periodic orbits and strange attractors) and stable attractors in the x-boundary Ricker dynamics (periodic orbits and strange attractors).

The eigenvalue governing the local transverse stability of an otherwise attracting periodic orbit of model (15) and (16) on the invariant manifold $y = 0$ is given by $\Pi_{n=1}^{n=N} a x_n e^{r(1-x_n)}$ where the set $\{x_n\}$ denotes all iterations of a periodic orbit and N denotes its period. If this eigenvalue is less than 1, then we say that the periodic orbit on the invariant manifold is transversally stable.

THEOREM 4.1   *If $a < 1$, then all periodic orbits on the invariant manifold $y = 0$ are transversally stable.*

Proof   Since $x_n e^{r(1-x_n)} = x_{n+1}$, we see that the transverse eigenvalue for a periodic orbit of period N is $\Pi_{n=1}^{n=N} a x_n$. At the equilibrium $x = 1$, the eigenvalue becomes a and hence the equilibrium is attractive in the y-direction for $a \leq 1$. It is known that for the Ricker map, the time average of cycles is identical to the positive fixed point [10]. An application of the inequality between arithmetic and geometric means yields

$$\left(\Pi_{n=1}^{n=N} a x_n\right)^{\frac{1}{N}} \leq \frac{1}{N} \sum_{n=1}^{n=N} a x_n = a,$$

implying that if $a < 1$, then all the period orbits on the invariant manifold $y = 0$ are transversally stable. ∎

Numerically, we find that, for $a < 1$ any set that is an attractor on the invariant manifold is transversally stable and hence a local attractor.

Figure 5 a–d shows an example of bistability between a period two orbit on the x-axis and a stable interior equilibrium. The Table 1 illustrates the different cases of bistable phenomena in regions 6 and 7 with $a = 1.5$ and r varying from $r < 2$ up to $r = 3.6$. Figure 6 shows the associated phase space dynamics.
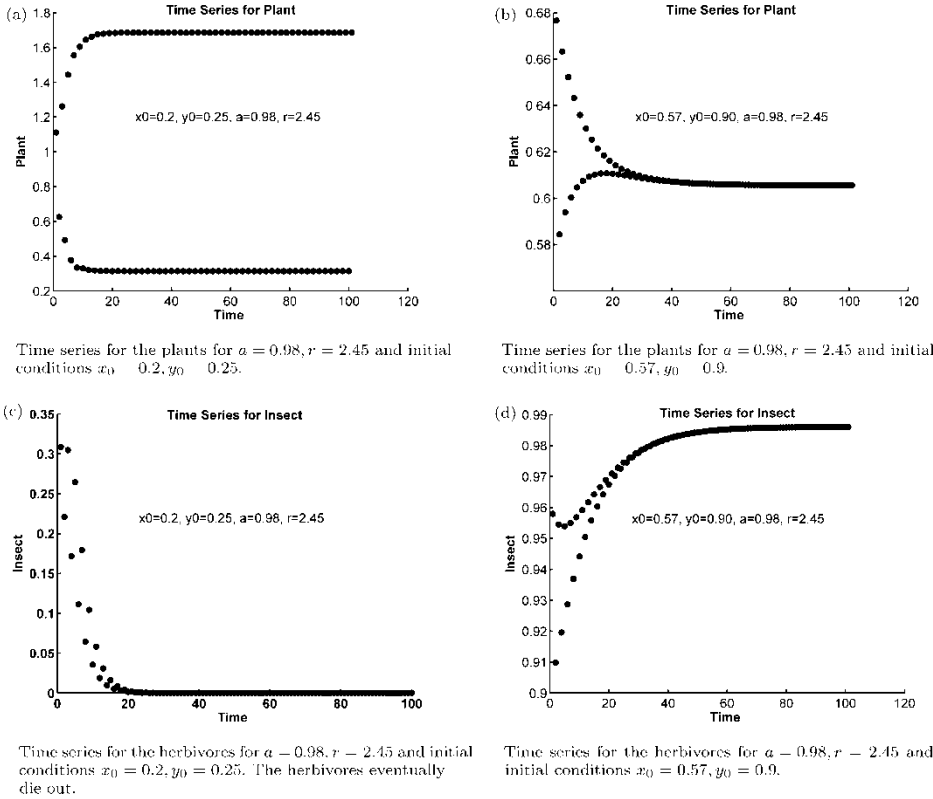
Dynamics of a plant-herbivore model

(a) Time series for the plants for $a = 0.98, r = 2.45$ and initial conditions $x_0 = 0.2, y_0 = 0.25$.

(b) Time series for the plants for $a = 0.98, r = 2.45$ and initial conditions $x_0 = 0.57, y_0 = 0.9$.

(c) Time series for the herbivores for $a = 0.98, r = 2.45$ and initial conditions $x_0 = 0.2, y_0 = 0.25$. The herbivores eventually die out.

(d) Time series for the herbivores for $a = 0.98, r = 2.45$ and initial conditions $x_0 = 0.57, y_0 = 0.9$.

Figure 5.   Bistability in region 3.

Table 1.   Bistability table.

Interior attractor *vs*. boundary attractor	Value of r	Value of a
Case 1. an invariant loop *vs*. period 2	2.6265	1.5
Case 2. an invariant loop *vs*. period 4	2.65	1.5
Case 3. period 21 *vs*. chaotic on x-axis	2.81	1.5
Case 4. period 6 *vs*. chaotic on x-axis	2.98	1.5

4.2.   *Strange attractor and its collapse*

Simulations in regions 4 and 6 show strange attractors. The small rectangles in Figure 2 are the result of a manual search for the stability boundary of the interior strange attractor. These points represent the values of a and r where the strange attractor collapses. The black curve connects these points. If the values of r or a are in region 5 in Figure 2, the strange attractor disappears and the population of y_n goes to zero.

Figure 7a–c gives an indication of how the strange attractor collapses. For $a = 0.95, r = 3.8$, we have bistability between two strange attractors, an interior one and a boundary one, *i.e.* the Ω-limit sets of some solutions with initial conditions in the interior are on the x-axis. The shaded set of Figure 7a is the interior strange attractor while the streaks of iteration points outside lie on the stable manifold of the strange attractor on the x-axis. It is highly likely that in the empty space between these two sets of trajectories there is a periodic orbit of saddle type with high period.

Yun Kang, Dieter Armbruster and Yang Kuang

Interior and boundary attractor for case 1 in Table 1.

Interior and boundary attractor for case 2 in Table 1.

Interior and boundary attractor for case 3 in Table 1.

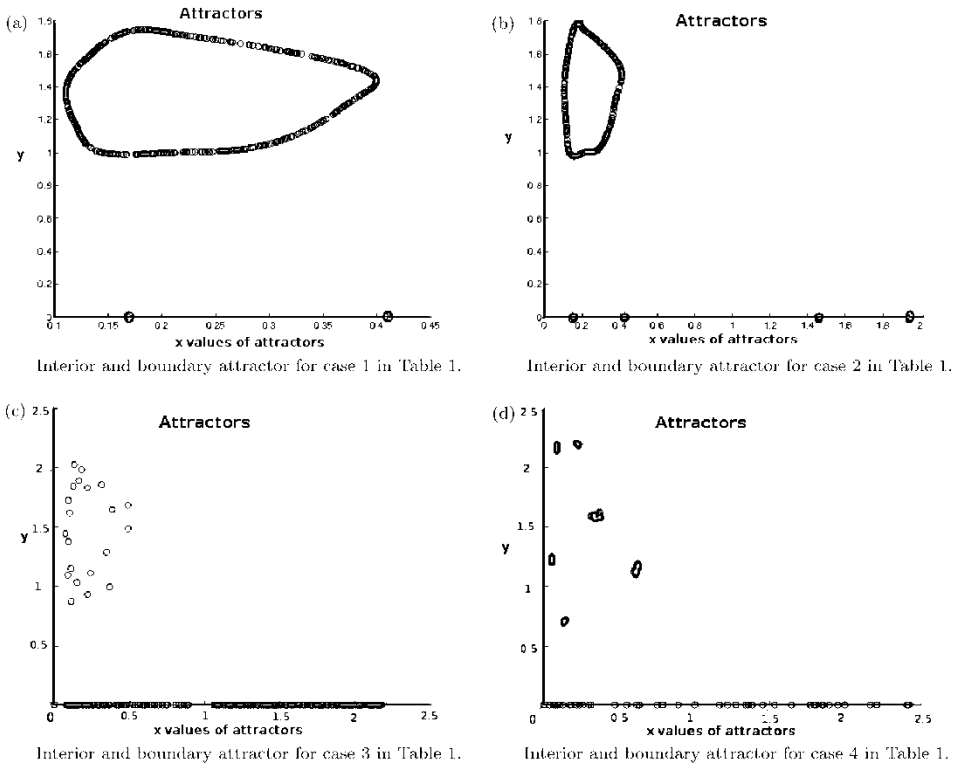Interior and boundary attractor for case 4 in Table 1.

Figure 6.   Bistability in regions 6 and 7.

As the interior strange attractor becomes larger (Figure 7b), it will collide with that unstable periodic orbit, leading to a 'leakage' of the strange attractor towards the x-axis in Figure 7c.

5.   Discussion

This paper considers a general plant–herbivore model, partly motivated by the dynamics of a gypsy moth infestation through biomass transfer from plants to the gypsy moth. Our discrete 2D model is controlled by the two parameters r, the nutrient uptake rate of the plant, and a the amount of leaves eaten by the herbivore. Mathematical analysis and simulations of this model provides us with biological insights that may be used to devise control strategies to regulate the population of the herbivore. Our results suggest the following two strategies:

(1) Exploiting *bistability*. In region 3, 4, 6 and 7 of Figure 2, the system shows bistability between attractors with nonzero population sizes for the herbivore corresponding to coexistence between plant and herbivore, and attractors on the x-axis corresponding to the extinction of the herbivores. Hence, if the population of the herbivores initially is small, it may eventually die out. This suggests control procedures to reduce the herbivore population by actions such as spraying of pesticides. Bistable dynamics is often generated in models through an explicit introduction of a threshold level below which the herbivore will die out regardless of the plant population levels. The bistability dynamics in our model (15) and (16) resulted from
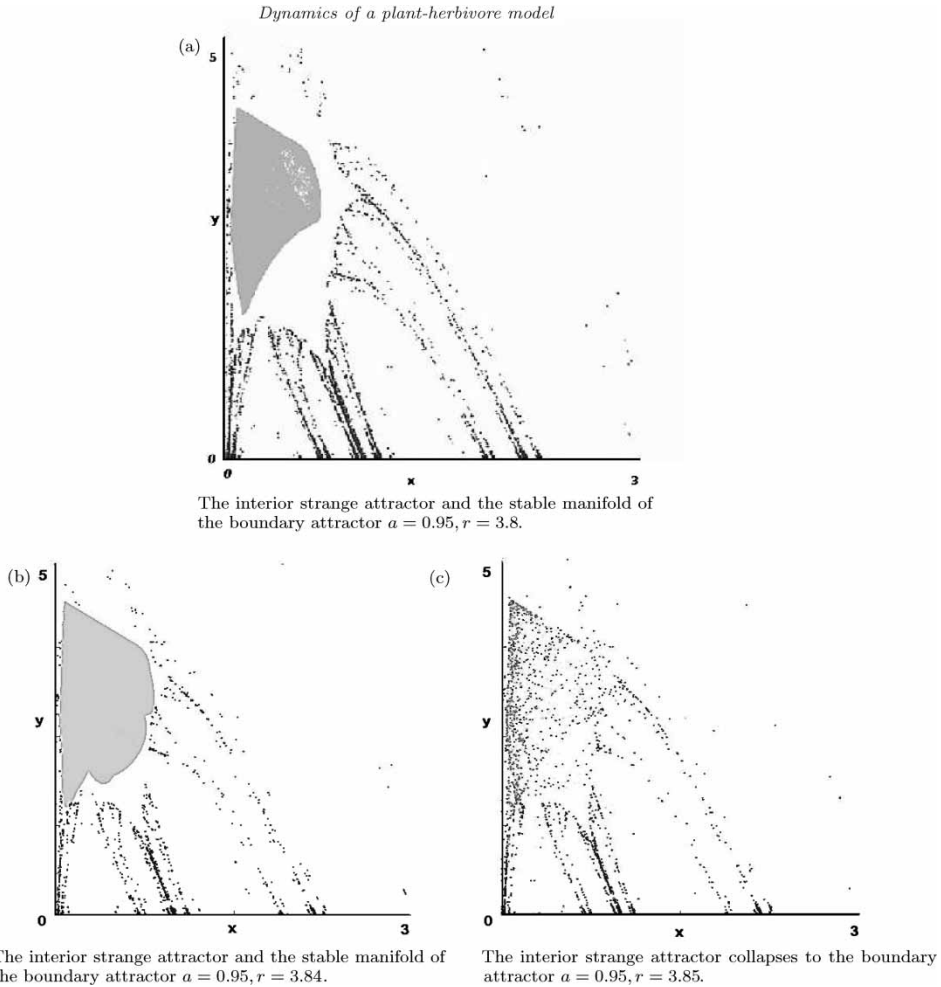
Figure 7.   How interior attractor collapses as *r* increases.

the intricate and plausible interaction of the plant and herbivore species. Namely, complex dynamics in a plant–herbivore model can lead to a multiple attractor case.

(2) Exploiting the *crisis of the strange attractor*. For all values of *a*, as the parameter *r* becomes large enough, the interior dynamics becomes unstable and all trajectories starting in the interior eventually approach the *x* axis, corresponding again to the extinction of the herbivore population. As *r* represents the growth rate of the plant species an increase could correspond to a natural occurrence of highly favourable growing conditions but also could be supported by fertilizing the plants. This seems to agree with the observation that herbivores such as gypsy moths produce outbreaks often in the year following some draught period and when plants suffer a period of sustained slow growth. Indeed, draught is regarded as the main culprit the severe gypsy moth outbreak in Maryland in summer 2007, US [18].

Acknowledgements

References

[1] K.C. Abbott and G. Dwyer, *Food limitation and insect outbreaks: Complex dynamics in plant-herbivore models*, preprint (2007), J. Animal Ecol. 76(5) (2007), pp. 1004–1014.

[2] J. Antonovics and D.A. Levin, *The ecological and genetic consequences of density-dependent regulation in plants*, Annu. Rev. Ecol. Syst. 11 (1980), pp. 411–452.

[3] J.R. Beddington, C.A. Free, and J.H. Lawton, *Dynamic complexity in predator-prey models framed in difference equations,* Nature 225 (1975), pp. 58–60.

[4] A.A. Berryman, *The theory and classification of out-breaks,* in *Insect Outbreaks*, P. Barbosa and J.C. Schultz, eds., Academic Press, New York, 1987, pp. 3–30.

[5] H. Caswell, *Matrix Population Models: Construction, Analysis and Interpretation,* 2nd ed., Sinauer Associates Inc., USA, 2006.

[6] M.J Crawley, *Herbivory: The Dynamics of Animal? Plant Interactions.* University of California Press, Los Angeles, CA, USA, 1983.

[7] L. Edelstein-Keshet, *Mathematical Models in Biology*, SIAM, Philadelphia, 2005.

[8] J. Guckenheimer, *Sensitive dependence on initial conditions for unimodal maps,* Commun. Math. Phys. 70 (1979), pp. 133–160.

[9] J.L. Harper, *Population Biology of Plants*, Academic Press, New York, 1977, pp. 1035–1039.

[10] R. Kon, *Multiple attractors in host-parasitoid interactions: Coexistence and extinction*, Math. Biosci. 201 (1–2) (2006), pp. 172–183.

[11] R.M. May, *Density dependence in host-parasitoid models*, J. Animal Ecol. 50 (1981), pp. 855–865.

[12] P.J. McNamee, J.M. McLeod, and C.S. Holling, *The structure and behaviour of defoliating insect/forest systems*. Res. Popul. Ecol. 23 (1981), pp. 280–298.

[13] A.J. Nicholson, *The balance of animal populations*, J. Animal Ecol. 2 (1933), pp. 131–178.

[14] A.J. Nicholson and V.A. Bailey, *The balance of animal populations. Part I*. Proc. Zoolog. Soc. Lond. 3 (1935), pp. 551–598.

[15] W.E. Ricker, *Stock and recruitment*, J. Fish. Res. Board Can. 11 (1954), pp. 559–623.

[16] A.R. Watkinson, *Density-dependence in single-species populations of plants*, J. Theor. Biol. 83 (1980), pp. 345–357.

[17] S. Wiggins, *Introduction to applied nonlinear dynamical systems and chaos*, 2nd ed., Springer, New York, 2002.

[18] http://www.mda.state.md.us/plants-pests/forest_pest_mgmt/gypsy_moth/current_conditions.php